OPEN

The ISME Journal (2017) 11, 1205–1217

www.nature.com/ismej

ORIGINAL ARTICLE

Syntrophic linkage between predatory *Carpediemonas* and specific prokaryotic populations

Emmo Hamann[1,2], Halina E Tegetmeyer[2,3], Dietmar Riedel[4], Sten Littmann[2], Soeren Ahmerkamp[2], Jianwei Chen[1,2], Philipp F Hach[2] and Marc Strous[1,2,3]

[1]*Department of Geoscience, University of Calgary, Calgary, AB, Canada;* [2]*Max Planck Institute for Marine Microbiology, Bremen, Germany;* [3]*Institute for Genome Research and Systems Biology, Center for Biotechnology, Bielefeld University, Bielefeld, Germany and* [4]*Max Planck Institute for Biophysical Chemistry, Göttingen, Germany*

Most anoxic environments are populated by small (<10 μm) heterotrophic eukaryotes that prey on different microbial community members. How predatory eukaryotes engage in beneficial interactions with other microbes has rarely been investigated so far. Here, we studied an example of such an interaction by cultivating the anerobic marine flagellate, *Carpediemonas frisia* sp. nov. (supergroup Excavata), with parts of its naturally associated microbiome. This microbiome consisted of so far uncultivated members of the Deltaproteobacteria, Bacteroidetes, Firmicutes, Verrucomicrobia and Nanoarchaeota. Using genome and transcriptome informed metabolic network modeling, we showed that *Carpediemonas* stimulated prokaryotic growth through the release of predigested biomolecules such as proteins, sugars, organic acids and hydrogen. Transcriptional gene activities suggested niche separation between biopolymer degrading Bacteroidetes, monomer utilizing Firmicutes and Nanoarchaeota and hydrogen oxidizing Deltaproteobacteria. An efficient metabolite exchange between the different community members appeared to be promoted by the formation of multispecies aggregates. Physiological experiments showed that *Carpediemonas* could also benefit from an association to these aggregates, as it facilitated the removal of inhibiting metabolites and increased the availability of prey bacteria. Taken together, our results provide a framework to understand how predatory microbial eukaryotes engage, across trophic levels, in beneficial interactions with specific prokaryotic populations.

The ISME Journal (2017) **11,** 1205–1217; doi:10.1038/ismej.2016.197; published online 17 February 2017

Introduction

Small heterotrophic eukaryotes (<10 μm) perform essential functions in marine ecosystems (Pernthaler, 2005; Edgcomb, 2016). For example, these eukaryotes capture and digest similar-sized microbes and release a mixture of nutrients, dissolved organic carbon and detritus to the environment, stimulating growth of prokaryotes. At the same time, microbial eukaryotes can become prey for the marine mesofauna and so link prokaryotic primary production to higher trophic levels (Sherr and Sherr, 2002).

In environments with high influxes of organic carbon, microbial activity often leads to a depletion of oxygen (Glud, 2008). Most eukaryotes cope with anoxia by switching from oxygen respiration to fermentation (Müller *et al.*, 2012; Stairs *et al.*, 2015). Just like in prokaryotes, fermentation in eukaryotes proceeds via glycolysis followed by the decarboxylation of pyruvate (Müller *et al.*, 2012). In strictly anerobic microbial eukaryotes, pyruvate decarboxylation often takes place in mitochondria that lost their capability to respire oxygen (Boxma *et al.*, 2005). These mitochondria recycle reducing equivalents by transferring electrons to organic metabolites or protons (H^+). Depending on the fermentation pathway used, this leads to the production of molecular hydrogen, fatty acids, alcohols and amino acids (Müller *et al.*, 2012).

In marine sediments, fermentation reactions may be syntrophically linked into a cascade of downstream metabolism, including respiration and further fermentation reactions (Fenchel and Jørgensen, 1977). This mediates a direct consumption of fermentation products and keeps their steady-state concentrations low. It is well established that such syntrophic interactions provide important bioenergetic advantages to prokaryotes (Sieber *et al.*, 2012). From the thermodynamic perspective, consumption of fermentation products enables fermentation reactions, which require low product concentrations.

Correspondence: E Hamann or M Strous, Department of Geoscience, University of Calgary, 2500 University Drive NW Calgary, AB, Canada T2N 1N4.
E-mail: emmohamann@gmail.com or mstrous@ucalgary.ca
Received 2 August 2016; revised 28 October 2016; accepted 7 December 2016; published online 17 February 2017

At low product concentrations, fermentative prokaryotes can maximize their growth efficiency and colonize environments with scarce energy resources (McInerney e*t al.* 2007). Among eukaryotes, similar nutritional interactions are found in ciliates or flagellates that harbor hydrogen-scavenging symbionts (van Hoek *et al.*, 2000; Boxma *et al.*, 2005; Ohkuma *et al.*, 2015). Parts of these symbionts might also be digested by their host, providing it with an additional carbon source. Yet, their main function appears to be the creation of a biochemical environment that favors fermentation reactions in the host's cytosol (Ohkuma *et al.*, 2015; Hamann *et al.,* 2016).

Even though symbiont-free eukaryotes are vital components of anerobic microbial communities (Edgcomb *et al.*, 2002; Wylezich and Jürgens, 2011), it has remained largely unaddressed how their physiological activity is affected by syntrophic interactions with free-living prokaryotes and vice versa. This prompted us to enrich the marine flagellate *Carpediemonas frisia* sp. nov. (Fornicata, supergroup Excavata), with part of its naturally associated bacterial and archaeal community. For this enrichment culture, we applied an experimental approach that combined physiological experiments with metabolic network modeling informed by genomics and transcriptomics. Our analysis focused on two main questions: (i) how do prokaryotes take advantage from the predatory behavior and metabolic activity of *C. frisia*? (ii) How does the biochemical activity of prokaryotes affect the fitness of *C. frisia*?

Materials and methods

Enrichment strategy

For the initial enrichment of *C. frisia*, we sampled sediment from the tidal flat 'Janssand' located in the German North Sea (53.73585N 7.69905 E, September 3, 2012). The samples were taken from a sulfidic sediment layer (located at 6 cm depth), which is known to host a rich diversity of sulfate-reducing and fermenting microorganisms (Gittel *et al.*, 2008; Dyksma *et al.*, 2016). The sediment was incubated in anoxic seawater medium (34 g l^{-1}, 1 mmol l^{-1} HEPES, pH = 8, Red Sea Deutschland, Germany) and supplemented with prey bacteria (10^9 cells ml^{-1}) as carbon source and sulfate (28 mM) as electron acceptor for bacterial respiration. As prey we used *Alteromonas macleodii* (strain ATCC 27126), a small, strictly aerobic bacterium that represents an abundant genus in the oxygenated water column *in situ* (García-Martínez *et al.*, 2002).

Growth of flagellates was monitored by regular microscopic inspection and by measuring the turbidity of the cultures. After an enrichment of flagellates was observed, a subsample of liquid culture was removed and grown in a sediment-free culture. This sediment-free culture was always transferred into fresh medium as soon as a depletion of bacterial prey was observed (within 4 to 5 days). Growth experiments and DNA/RNA sequencing were conducted after 26 days (after five culture transfers).

Microscopy

For transmission electron microscopy, the cells were collected with a table top centrifuge at 2000 r.p.m. (Stat Spin Microprep 2). After centrifugation, the pelleted sample was vitrified in a high-pressure freezer (BAL-TEC HPM-010). Substitution was carried out at − 90 °C with 0.1% tannic acid in anhydrous acetone for 24 h, and for an additional 8 h in 2% OsO_4 in anhydrous acetone. After a further incubation over 20 h at − 2 °C, the samples were warmed up to +4 °C and washed with anhydrous acetone. The samples were embedded at room temperature in Agar 100 (Epon 812 equivalent) at 60 °C for 24 h. After thin sectioning (60 nm), the sections were counter-stained with lead citrate. The samples were analyzed with a Philips CM 120 transmission electron microscope (Philips Inc., Eindhoven, The Netherlands). Images were taken with a TemCam F416 CMOS camera (TVIPS, Gauting, Germany).

For scanning electron microscopy, the cells were centrifuged at 400 r.p.m. for 6 min, collected and placed on teflon slides for 5 min. The cells were then fixed with 2% glutaraldehyde solution (in 34 g l^{-1} sterile seawater, 1 mM HEPES, pH = 8) for 60 min at room temperature. Fixation was followed by a washing step in deionized water and ethanol dehydration in 30%, 50%, 70%, 90% and 100% ethanol (20 min each). Before microscopic evaluation, the specimens were subjected to critical point drying with CO_2 (Leica EM CPD300, Leica, Wetzlar, Germany). Imaging was performed with a nova NanoLab 600 scanning electron microscope (FEI Company, Eindhoven, The Netherlands).

For fluorescence microscopy, the cells were fixed in 1.8% formaldehyde solution (2 h) and stained with the DNA specific stain 4',6-diamidino-2-phenylindole (DAPI 1 μg ml^{-1}, 3 min, at 37 °C). Pictures were taken with an epifluorescence microscope (Leila DM: Osram centra mercury-vapor lamp) connected to an AxioCam MRm camera (Carl Zeiss, Jena, Germany).

Mitochondria-related organelles were stained with MitoTracker (Red CMXRos) according to the manufacturer's protocol (Thermo Fisher Scientific GmbH, Dreieich, Germany).

Next-generation sequencing, binning and quality control

The samples for DNA and RNA were retrieved from an exponentially growing culture in mid-exponential phase and subjected to next-generation sequencing. For this, biomass was harvested from an enrichment culture that had been transferred five times. DNA and RNA extraction was performed as previously described (Smith *et al.*, 2007). For DNA sequencing, a Nextera

mate pair library and a PCR-free shotgun library were constructed from genomic DNA and sequenced on an Illumina MiSeq Sequencing System (Illumina, San Diego, CA, USA). This yielded 11.8 million mate pair reads and 16.8 million paired-end reads after quality trimming. Both trimmed read sets had an average read length of 250 bp. In addition, RNA was prepared for sequencing in two separate approaches. One library was prepared according to the Illumina TruSeq RNA Sample Preparation v2 Guide, using poly-T oligo-attached magnetic beads to enrich eukaryotic mRNA. A second library was prepared by depletion of prokaryotic rRNA (Ribo-Zero Kit for Bacteria, epicenter) without enrichment of eukaryotic mRNA. Both mRNA libraries were sequenced on a MiSeq instrument yielding 3.6 million poly-A tail enriched paired-end reads and 24.7 million non-enriched paired-end reads after quality trimming. Both trimmed read sets had an average read length of 75 bp. Genomic reads were quality trimmed and filtered using nesoni (https://github.com/Victorian-Bioinformatics-Consortium/nesoni) and NextClip (Leggett *et al.*, 2014). Assembly of the quality filtered reads was done with SPAdes (Bankevich *et al.* 2012). Genomes were binned based on % GC, tetranucleotide composition and sequence coverage using Metawatt (Strous *et al.*, 2012). Genome completeness for prokaryotic bins was evaluated with CheckM (Parks *et al.*, 2015) using the implemented conserved reference gene sets. Genome completeness for the eukaryotic bin was estimated by searching for the presence of 169 conserved eukaryotic genes as previously described (Hamann *et al.*, 2016). All sequence data for this project are publicly available at the National Center for Biotechnology Information with the accession numbers SRX2012078-SRX2012079, SRR4448896-SRR4448897 (high-throughput DNA and RNA sequence read archive). The Sanger-sequenced eukaryotic SSU rDNA gene was submitted to GenBank (accession no. KY031954).

Gene annotation and prediction of syntrophic linkages

Gene predictions and functional annotations for the prokaryotic populations were done with the RAST online annotation pipeline (Glass *et al.*, 2010). For the eukaryotic genome, structural annotations and gene predictions were performed with the MAKER pipeline (Cantarel *et al.*, 2008). After an initial *ab initio* gene prediction with GeneMark-ES (Ter-Hovhannisyan *et al.*, 2008), we refined the obtained gene models with evidence-driven gene predictions using snap (Korf, 2004). As evidence, we used 14 190 assembled transcripts (5.5 Mb) of a poly-A-tail enriched transcriptome (see above). Repeat identification, annotation and masking were done with RepeatMasker (Smit *et al.*, 2013). Genes for the core metabolism were manually identified by blastx and blastp homology searches against the UniProtKB/Swiss-Prot protein database. Translocation of gene products to mitochondria-related organelles was predicted based on the presence of N-terminal target peptides using TargetP (Emanuelsson *et al.*, 2007). Protein architectures and conserved protein domains were identified using the Pfam (Finn *et al.*, 2014) and the SMART (Letunic *et al.*, 2015) protein domain detection tools.

Metabolic linkages between different microbial populations were predicted based on transcriptional activities of each gene of each population. Genes involved in energy and carbon metabolism were identified based on the RAST annotations and ranked according to their transcriptional activity. Transcriptional gene activities were estimated by calculating the sum of all mapped mRNA reads per gene, divided by the length of each gene. Mapping and read counting was performed using bbmap (http://sourceforge.net/projects/bbmap/) and samtools (http://samtools.sourceforge.net/). For the prokaryotic populations, only metabolic pathways that had transcription levels above the per-population average gene activity were included into the metabolic network. Syntrophic linkages between different populations were inferred by identifying metabolites that were predicted to be a substrate for one population and a metabolic end product of another population.

Phylogenetic analysis

To evaluate the phylogeny of the enriched microbial populations each genomic bin was screened for the presence of SSU rRNA sequences using HMMER (Finn *et al.*, 2015). The retrieved sequences were then blasted to the NCBI database and closely related sequences were downloaded for phylogenetic tree calculation. Gene alignments were calculated with MAFFT (Katoh and Standley, 2013). Phylogenetic trees were constructed with RAxML (Stamatakis, 2014) using the GTR+GAMMA model with 400 rapid bootstrap iterations followed by a search for the best scoring maximum-likelihood tree. For the flagellate, we calculated a separate tree based on a multigene alignment consisting of six universal eukaryotic genes (Takishita *et al.*, 2012). For this tree, the amino acid partitions were calculated with the WAG replacement matrix with maximum-likelihood estimated base frequencies at 400 rapid bootstrap iterations.

Physiological experiments and wet lab chemistry

To determine the influence of interspecies hydrogen transfer on the fitness of *C. frisia*, four cultures were grown in parallel until they reached the early exponential phase. The cultures were then supplied with ^{13}C-labeled *Alteromonas* to monitor organic carbon remineralization rates (production of $^{13}CO_2$ from ^{13}C biomass). Shortly afterwards, the sulfate-reducing activity in two cultures was inhibited with 2 mM of sodium molybdate, a competitive inhibitor of sulfate reduction (Oremland and Capone, 1988).

$^{13}CO_2$ production, hydrogen concentration and eukaryotic cell numbers were recorded (in time steps of 6 min) to monitor the immediate effect of hydrogen accumulation on the microbial activity.

For the determination of protist abundance, 50 µl subsamples of liquid culture was removed from the bottles, mixed with formaldehyde solution to a final concentration of 0.02% to immobilize the swimming cells. The cell abundance was determined by manually counting with an improved Neubauer counting chamber (BRAND counting chamber, Neubauer improved, 0.1 mm depth).

To monitor the respiration rates (production of $^{13}CO_2$ from ^{13}C-labeled biomass), liquid samples (1 ml) were filled into exetainers and 0.2% zinc acetate solution was added to abolish microbial activity. The isotopic component of DIC was determined after acidifying with 1% (final) hypophosphoric acid on a gas chromatography isotope ratio monitoring mass spectrometer (Optima Micromass, Manchester, UK).

Volatile fatty acids were measured with a Syham HPLC system (Fürstenfeldbruck, Germany) equipped with an Aminex HPX-87 H HPLC column (300 × 7.8 mm) and 5 mM H_2SO_4 as eluent. Separation was performed in isothermal mode at 40 °C and the eluted compounds were simultaneously detected with an ultraviolet and a refractive index detector at a detection limit of 0.1 mM. As calibration standard, a mixture of the fatty acids succinate, lactate, formate, acetate, propionate and butyrate was measured at different concentrations.

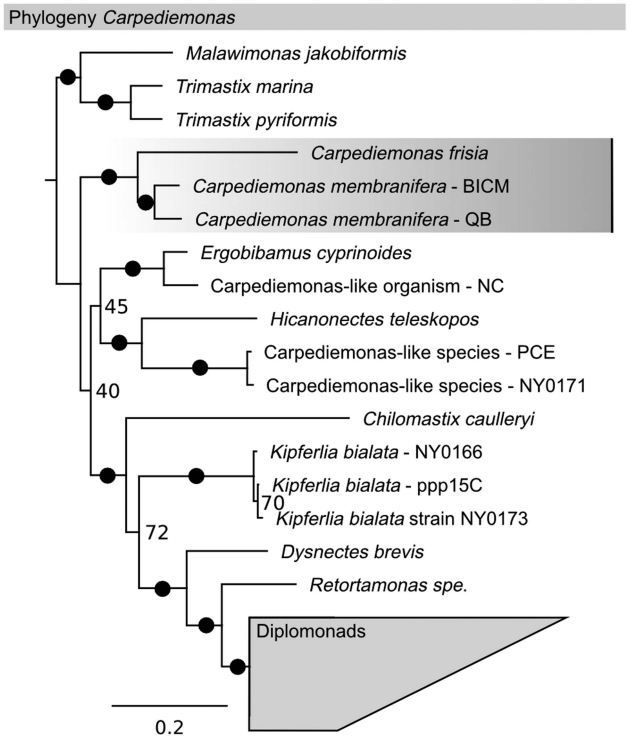

Figure 1 Phylogeny of *C. frisia* and related Excavata. The phylogenetic tree was inferred from a multigene alignment of six universal eukaryotic genes and calculated by RAxML. The Diplomonads comprise the genera *Trichomonas* and *Giardia*. The scale bar represents substitutions per side. Numbers represent %-bootstrap support values. Circles indicate 100% support.

Results

Enrichment of C. frisia and its associated microbiota

We stimulated growth of predatory flagellates and prokaryotes by anerobically incubating marine sediment with prey bacteria as the only carbon source and sulfate as the only electron acceptor. Light microscopy indicated growth of flagellates and indigenous bacteria after 3 days of incubation. We cultivated a subsample of the enrichment culture in sediment-free medium and repeatedly transferred it every 4 to 5 days. After four transfers, a morphologically uniform population of flagellates was observed. PCR amplification and Sanger sequencing of 18S rRNA genes confirmed the presence of a single eukaryotic phylotype. Phylogenetic analysis placed this phylotype in a well-supported clade within Fornicata (supergroup Excavata; Figure 1). *Carpediemonas membranifera* was its closest cultivated relative (94% sequence identity of the 18S rRNA gene). Consistently, electron microscopy confirmed the presence of all morphological features typical for excavate flagellates (Figure 2, Supplementary Figure 1). We designated the flagellate as the novel species *Carpediemonas frisia* (see below for a formal description). *C. frisia* is a biflagellated protist that preys on suspended bacteria by using a beating anterior flagellum that directs prey bacteria towards the cell. Ingestion of bacteria into membrane-enclosed digestive vacuoles took place at the ventral feeding groove. In these vacuoles, bacteria appeared to be only incompletely digested as shown by the accumulation of membrane remnants and other high molecular weight material (Figure 2d, Supplementary Figures 1a–c). Transmission electron microscopy also revealed the presence of mitochondria-related organelles with slight membrane folding (Figure 2f). Staining with mitotracker, a dye retained in the presence of an active membrane potential, showed positive signals, indicating physiological activity of these organelles (Figure 2e).

Microscopic observation further indicated that a morphologically diverse prokaryotic community was co-enriched with *C. frisia*. Prokaryotes were often associated with aggregates. Aggregation appeared to be supported by the formation of a network of pili and extracellular material (Figure 2a). *C. frisia* itself was frequently found associated to these aggregates.

Microbial community structure and communal metabolism

After we confirmed that *C. frisia* was the only eukaryotic species in the culture, we determined the

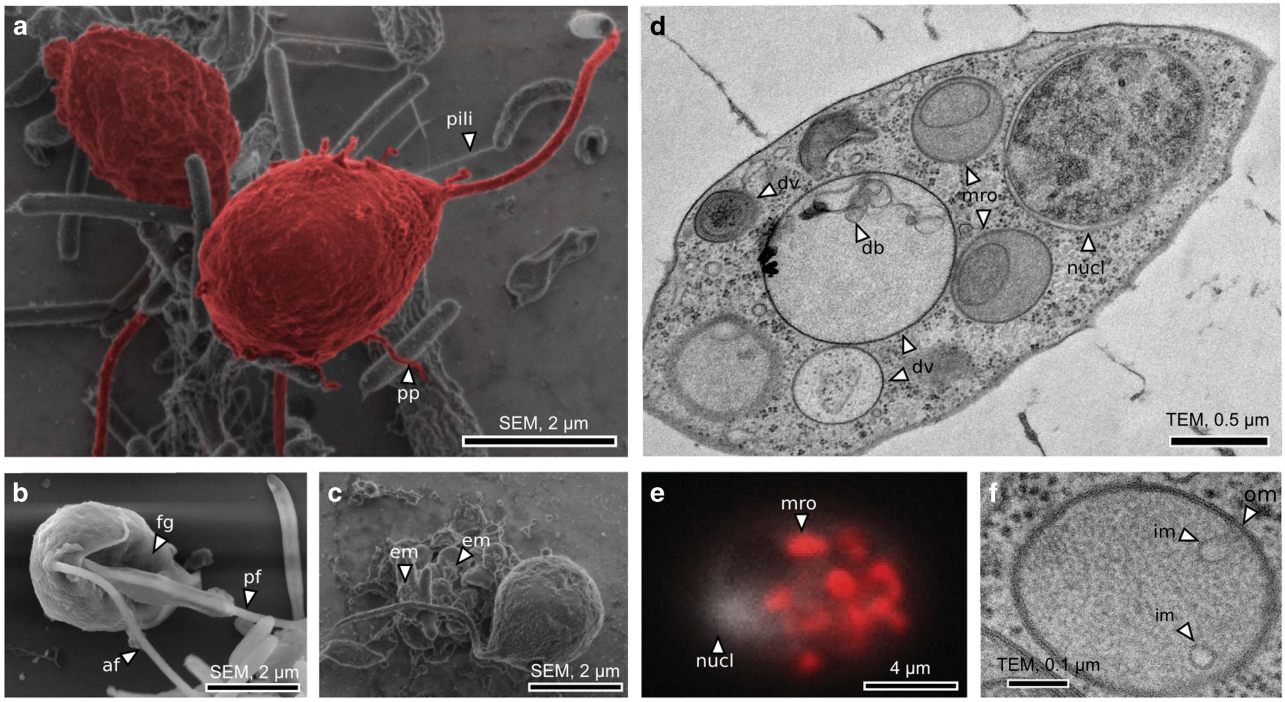

Figure 2 Microscopic images of *C. frisia* and associated prokaryotes. (**a–c**) Scanning electron images of *C. frisia*. *C. frisia* was often found in close proximity to prokaryotic aggregates. Arrows indicate pili (pili), pseudopodia (pp), anterior flagellum (af), posterior flagellum (pf), feeding groove (fg) and extracellular material (em). (**d**) Transmission electron micrograph of *C. frisia*. The arrows indicate digestive vacuoles (dv), mitochondria-related organelles (mro), the nucleus (nucl) and incompletely digested organic material (db). (**e**) Mitotracker staining of branching mitochondria-related organelles. (**f**) Close-up of a mitochondria-related organelle showing inner (im) and outer membrane (om) as well as slight membrane folding.

ecological functions of the individual community members. For this, DNA and RNA was extracted from the exponentially growing culture and subjected to next-generation sequencing. The genomic reads were assembled and binned, resulting in provisional whole genome sequences for all abundant microbial populations (Figure 3). For prokaryotes, the genome completeness and quality was estimated with CheckM (Parks *et al*., 2015). For *C. frisia* genome completeness was estimated by searching for the presence of conserved eukaryotic marker genes (Hamann *et al*., 2016). The results are shown in Table 1.

The genomes belonged to *C. frisia* itself and members of Deltaproteobacteria, Bacteroidetes, Firmicutes, Verrucomicrobia and Archaea. Based on the annotated genomes and transcriptional activities, we reconstructed the core metabolism of these populations. The genomes of the subpopulations of Deltaproteobacteria, Bacteroidetes and Firmicutes encoded for very similar metabolic capabilities. Therefore, we treated them as single ecological guilds in our analysis. The predicted metabolic interactions of *C. frisia* with these guilds are shown in Figure 4.

For *C. frisia*, we recovered a 12.38 MB provisional genome with an estimated completeness of 93%. We predicted 5695 protein-coding genes, covering 59% of the genome. The free-living, predatory lifestyle of *C. frisia* was well reflected in its genome. *C. frisia* encoded typical features for actin-based phagotrophy, motility and the ability to use hydrolysis products from ingested bacteria. *C. frisia* also encoded genes for an exocytosis machinery, supporting the excretion of undigested particles and other substances through secretory vesicles. Consistent with the known physiological capabilities of the related genera *Trichomonas* and *Giardia* (Müller *et al*., 2012), *C. frisia* lacked the capability for autotrophy, oxygen respiration and proton-driven adenosine triphophate (ATP) synthesis (Figure 4b). Instead, it was inferred to depend on the use of carbohydrates and amino acids to drive a strictly fermentative metabolism. Transcriptional gene activities indicated that ATP production was coupled to glycolysis followed by the decarboxylation of pyruvate. Pyruvate decarboxylation appeared to be catalyzed by the subsequent activity of pyruvate:ferredoxin oxidoreductase and acetyl-CoA synthetase. Further, we detected transcriptional activity of a Fe-hydrogenase and the NADH oxidizing subunits (NouE/NuoF) of respiratory Complex I (Supplementary Figure 2). The combined activity of these enzymes is known to catalyze the proton dependent, simultaneous ('confurcating') re-oxidation of NADH and reduced ferredoxin, leading to the production of hydrogen ('H_2'). In addition, *C. frisia* was inferred to be capable of the re-oxidation of NADH through the activity of lactate and/or alcohol dehydrogenases. We also checked for the presence of N-terminal target peptides that support translocation of gene products to the

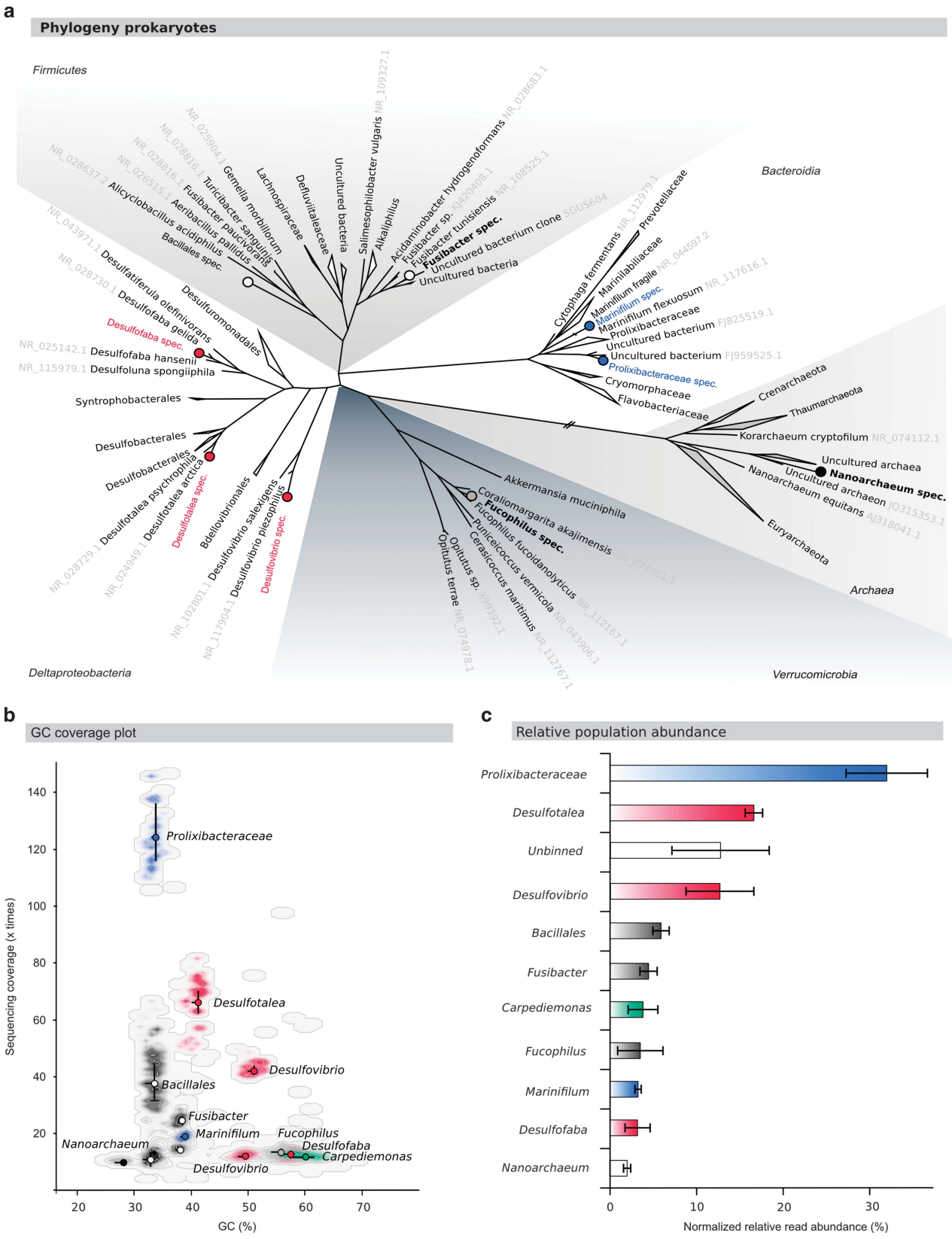

Figure 3 Phylogeny and relative abundances of the enriched prokaryotic populations. (**a**) Phylogenetic tree based on a 16S rRNA gene alignment as inferred by RAxML. Colored dots indicate species co-enriched with *C. frisia*. The scale bar indicates substitution per site. (**b**) GC/coverage plot for *C. frisia* and co-enriched prokaryotic populations. (**c**) Relative population sizes based on normalized sequence read counts per prokaryotic population. The reads were obtained from two different sequence libraries. The error bar indicates the standard deviation.

Table 1 Genome statistics for the binned prokaryotic and eukaryotic populations and quality control statistics

Bin	*Sequence size*	*No. contigs*	*% GC*	*Shortest contig*	*Mean sequence size*	*Longest contig*	*N50*
Genome statistics for the binned prokaryotic and eukaryotic populations							
Prolixibacteraceae	4 292 540	45	32.4	537	95 389.8	1 448 797	505 417
Marinifilum	7 836 933	1089	37.8	601	7196.4	1 053 175	150 714
Fusibacter	14 684 666	411	37.3	511	35 729.1	641 269	190 630
Fucophilus	4 491 245	124	54.3	627	36 219.7	3 997 856	3 993 360
Desulfovibrio	3 776 536	24	49.9	507	157 355.7	1 377 773	1 119 696
Desulfotalea	4 344 744	141	39.7	501	30 813.8	773 452	260 248
Desulfofaba	8 603 717	374	56.1	516	23 004.6	357581	5 4841
Carpediemonas	12 382 280	2326	58.6	500	5323.4	5 8509	9593
Bacillales	19 354 553	3057	32.3	500	6331.2	1 002 323	3 0666
Archaea	1 747 950	555	27	522	3149.5	6 1962	1 2541

Bin	*Marker lineage*	*No. of genomes*	*No. of markers*	*No. of marker sets*	*% Completeness*	*Contaminations*	*Strain heterogeneity*
Quality control statistics							
Prolixibacteraceae	Bacteroidetes	419	286	195	97.95	3.08	0
Marinifilum	Bacteroidetes	419	286	195	95.9	66.9	0.52
Fusibacter	Clostridia	446	196	110	100	206.57	4.98
Fucophilus	Verrucomicrobia	12	346	245	99.59	6.71	0
Desulfovibrio	Deltaproteobacteria	93	197	125	96.66	0	0
Desulfotalea	Deltaproteobacteria	93	197	125	99.6	6.78	7.32
Desulfofaba	Deltaproteobacteria	93	197	125	96	2.6	0
Bacilliales	Bacilli	821	250	136	96.69	449.99	3.3
Archaea	Archaea	207	149	107	72.9	4.67	14.29

The marker lineages indicate the taxonomic rank of the lineage-specific marker set used to estimate quality control statistics. Genome completeness was estimated from the presence/absence of lineage specific marker genes. Contaminations were determined by the presence of multi-copy marker genes and the expected collocalization of these genes. Strain heterogeneity was determined by the number of multi-copy marker, which exceed a specified amino acid identity threshold. (See also Parks *et al.* (2015) for detailed explanation).

mitochondria-related organelles. None of the predicted genes involved in *C. frisia's* energy metabolism contained such target peptides. Thus, energy conservation in *C. frisia* appears to take place entirely in the cytosol.

Bacteroidetes was the most abundant group of bacteria co-cultured with *C. frisia*. Bacteroidetes were represented by two different populations. One population was affiliated to the genus *Marinifilum* (7.8 MB, 96% complete) and another was most closely related to a group of deeply branching, so far uncultivated Prolixibacteraceae (4.3 MB, 98% complete). The latter appeared to be most abundant, with a relative abundance of 33% as estimated by normalized read counts. (Figure 3c). From previous studies, it is known that Bacteroidetes are specialized consumers of high molecular weight compounds such as proteins and polysaccharides (Fernández-Gómez *et al.*, 2013). To break down these compounds Bacteroidetes make use of a variety of specialized transporters and enzymes with hydrolytic activity (Bauer *et al.*, 2006). The Prolixibacteraceae population detected here, also displayed high activity of these enzymes. Specifically, we recorded high transcriptional activity of genes encoding for proteases, glycoside hydrolases, and glycosyltransferases (Supplementary Figure 3). In addition, activity of TonB-dependent and ABC-like biopolymer transport systems indicated the consumption of macromolecular organic material (Supplementary Figure 5). Energy appeared to be conserved by fermentation as shown by high transcriptional activity of genes involved in glycolysis. In addition, genes encoding for acetyl-CoA synthetase, acetate kinase and Fe-hydrogenases showed high transcriptional activity. Taken together, both Bacteroidetes populations were inferred to belong to the same ecological guild that performed biopolymer degradation and fermentation with hydrogen and acetate as main metabolic end products.

In addition to Bacteroidetes, we also recovered genomes for two major populations of Firmicutes belonging to the genera *Fusibacter* (14.7 MB, 100% complete) and *Bacillus* (19.4 MB, 97% complete). Both populations consisted of several subpopulations exhibiting different degrees of genetic heterogeneity, as indicated by the detection of multiple single copy marker genes and the large bin sizes (Table 1).

Together, all Firmicutes were estimated to make up about 12% of the total microbial community. They were inferred to consume a broad range of biomolecules including amino acids, sugars and other low molecular weight organic acids. This was indicated by high transcriptional activity of genes encoding for oligopeptide, nucleoside and sugar ABC-like transporters as well as TRAP-like C4-dicarboxylate transporters (Supplementary Figures 3 and 4).

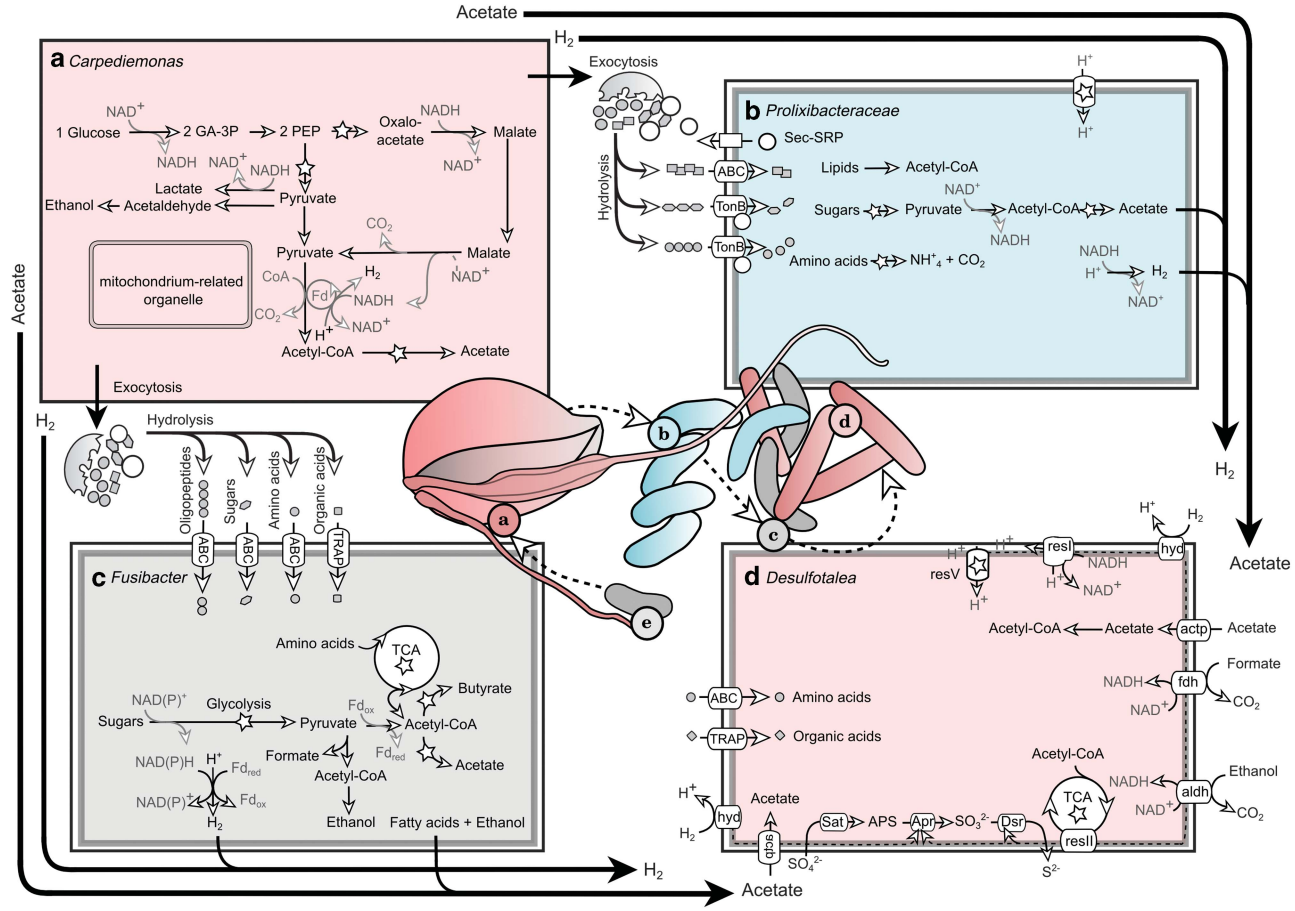

Figure 4 Metabolism of *C. frisia* and co-enriched prokaryotes. (**a**–**d**) Communal metabolism of *C. frisia* and co-enriched prokaryotes as inferred from genomic and transcriptomic sequencing. Each organism represents its ecological guild in the metabolic network. *C. frisia* (**a**) captures and digests particulate food bacteria (**e**) that were supplemented to the culture. *C. frisia* stimulated growth of prokaryotes through the release of hydrogen, acetate and incompletely digested macromolecular material. The processing of macromolecular material appeared to be mainly performed by Bacteroidetes (**b**) and Firmicutes (**c**). Deltaproteobacteria (**d**) were inferred to consume hydrogen, alcohols and fatty acids.

These substrates were predicted to be fermented to butyrate, acetate, formate, ethanol and hydrogen. Hydrogen production in Firmicutes appeared to proceed via the same mechanism as in *C. frisia,* through the simultaneous oxidation of NADH and reduced ferredoxin. This was indicated by transcriptional activity of genes encoding for Fe-hydrogenases and the NADH oxidizing subunits of respiratory Complex I (Supplementary Figure 2). These genes were encoded in a single operon. In sum, all Firmicutes were inferred to perform very similar functions by metabolizing low molecular weight biomolecules in a fermentative catabolism.

The remainder of the bacterial community mainly consisted of Deltaproteobacteria. Phylogenetic analyses showed that Deltaproteobacteria were present as three main populations belonging to the genera *Desulfotalea* (4.3 MB, 100% complete), *Desulfovibrio* (3.8 MB, 97% complete) and *Desulfofaba* (8.6 MB, 96% complete). Together, these populations made up approximately 30% of the total microbial community. The encoded core metabolisms of these populations indicated that they were mainly involved in the consumption of hydrogen and other fermentation products. Specifically, we found high activities of genes supporting the uptake of short chain fatty acids and amino acids, as well as the oxidation of hydrogen. Hydrogen consumption was catalyzed by a high-affinity Ni/Fe-hydrogenase and coupled to a membrane-bound respiratory chain that used sulfate as terminal electron acceptor. In addition, all Deltaproteobacteria populations transcribed genes encoding for type IV pilus assembly proteins and the fimbria forming protein pilin. This was in agreement with observations made via scanning electron microscopy, which suggested the presence of pili-like structures aiding in aggregation of prokaryotes (compare Figure 2).

Apart from the major bacterial populations, we also detected a small population of Verrucomicrobia and Archaea. 16S rDNA gene phylogenies showed that the detected population of Verrucomicrobia was related to the genus *Fucuphilus*. Similar to the Firmicutes, this population was involved in the

uptake and fermentation of sugar monomers and amino acids. The archael population was related to a clade of so far uncultivated species from mesophilic and thermophilic marine environments. The closest isolated and described relative was *Nanoarchaeum equitans*. This species is known for its reduced genome size, limited metabolic capabilities and an epibiotic association with the archaeum *Ignicoccus* (Waters *et al.*, 2003). The archaeal genome recovered here was also small (1.75 Mb) and encoded only basic metabolic capabilities. The most basic requirements to sustain life appeared to be present given the detection of genes for ATP synthesis, DNA replication, transcription and translation. Based on its encoded core catabolism, the archaeon appeared to be dependent on a fermentative metabolism. Transcriptional activities of genes encoding for a sugar ABC-like transporter, a pyruvate kinase and an acetate kinase indicated an involvement in the fermentation of sugar monomers. In addition, activity of genes encoding for a methyl-accepting chemotaxis protein and archaeal flagellin were detected. Genes supporting methanogenesis, hydrogen oxidation, sulfur oxidation or ammonium oxidation, were not detected.

Relevance of syntrophy for the fitness of C. frisia

Our metagenomic and transcriptomic analyses suggested that fermentation in *C. frisia* was facilitated by interspecies hydrogen transport from *C. frisia* to sulfate-reducing *Desulfotalea, Desulfovibrio and Desulfofaba*. To confirm this inference experimentally, molybdate, a competitive inhibitor of sulfate reduction, was added to the exponentially growing *C. frisia* enrichment culture (Figure 5). For this experiment, we used ^{13}C-labeled prey bacteria and monitored their consumption and conversion by the analysis of produced $^{13}CO_2$. Immediately after inhibition of sulfate reduction, we observed a rapid accumulation of hydrogen in the culture (Figure 5c). In addition, we observed an accumulation of butyrate, formate and acetate (Supplementary Figure 6b). Growth of *C. frisia* completely stopped shortly after the onset of hydrogen accumulation (Figure 5a). Concomitantly, $^{13}CO_2$ production rates leveled off compared with the control. In addition, we incubated *C. frisia* in medium containing only limiting amounts of sulfate (200 μM). This cultivation condition favored the growth of fermenting species but did not support hydrogen oxidation coupled to sulfate reduction. Also, for this treatment, we observed a significantly reduced growth rate and growth yield of *C. frisia* (Supplementary Figures 6c and d).

Discussion

In this study, we showed that anoxic incubation of a marine sediment supplemented with prey bacteria as carbon source and sulfate as electron acceptor led to the enrichment of the predatory protist *C. frisia* and co-enrichment of a prokaryotic community. After five subsequent culture transfers in sediment-free medium, this community consisted of distinct populations affiliated with Bacteroidetes, Firmicutes, Deltaproteobacteria, Verrucomicrobia and Nanoarchaeota. Metabolic interactions were inferred from the analysis of metagenomic and transcriptomic sequence data. *C. frisia* appeared to provide two major nutritional opportunities for prokaryotes: First, the degradation of incompletely digested macromolecular organic material and second, the oxidation of sugars, organic acids and hydrogen with sulfate. Physiological experiments confirmed that the fitness of *C. frisia* was directly impacted by the hydrogen oxidizing activity of Deltaproteobacteria.

Our genomic and transcriptomic analysis suggested that *C. frisia* produced hydrogen through the simultaneous (confurcating) oxidation of NAD(P)H and ferredoxin using an enzyme complex that consisted of the catalytic subunits of respiratory Complex I (NouE/ NuoF) and a Fe-hydrogenase. This reaction is very common among fermentative bacteria (Schut and Adams, 2009) and has also been predicted to be used by a variety of eukaryotic species (Stairs *et al.* 2015). However, the available free energy released during NAD(P)H-dependent hydrogen production decreases exponentially with increasing product concentration. For the synergistic production of molecular hydrogen from NAD(P)H and ferredoxin to proceed, the maximum hydrogen concentration is 0.1 mM (at $NADH/NAD^+ = 10$; Stams and Plugge, 2009). Many fermenting eukaryotes have evolved symbiotic relationships with hydrogen-scavenging prokaryotes, which allow them to maintain intracellular hydrogen levels below this threshold. For example, ciliates and amoeba often harbor hydrogen-consuming methanogens inside their cytosol (van Bruggen *et al.*, 1985; van Hoek *et al.*, 2000; Boxma *et al.*, 2005).

Another example is the breviate *Lenisia limosa*, which forms epibiotic associations with hydrogen oxidizing *Arcobacter* (Hamann *et al.*, 2016). In this association, the maximum hydrogen concentration has been reported to be 20 times lower than predicted for *C. frisia*. This can be explained by the observation that *L. limosa* mainly uses NAD(P)H for hydrogen production, a reaction that is more prone to product inhibition than the simultaneous oxidation of NAD(P)H and ferredoxin. This may also explain why *C. frisia* can sustain its metabolism without the tight symbiotic association observed for *L. limosa* and other hydrogen-producing eukaryotes. In any case, if the maximum hydrogen concentration is exceeded, NAD(P)H needs to be re-oxidized by reduction of organic metabolites such as pyruvate or succinate. Less energy is conserved in this metabolic bypass, leading to a reduced growth efficiency. In addition, NAD(P)H-dependent pyruvate oxidation may lead to the production of ethanol and acetaldehyde (Müller *et al.*, 2012),

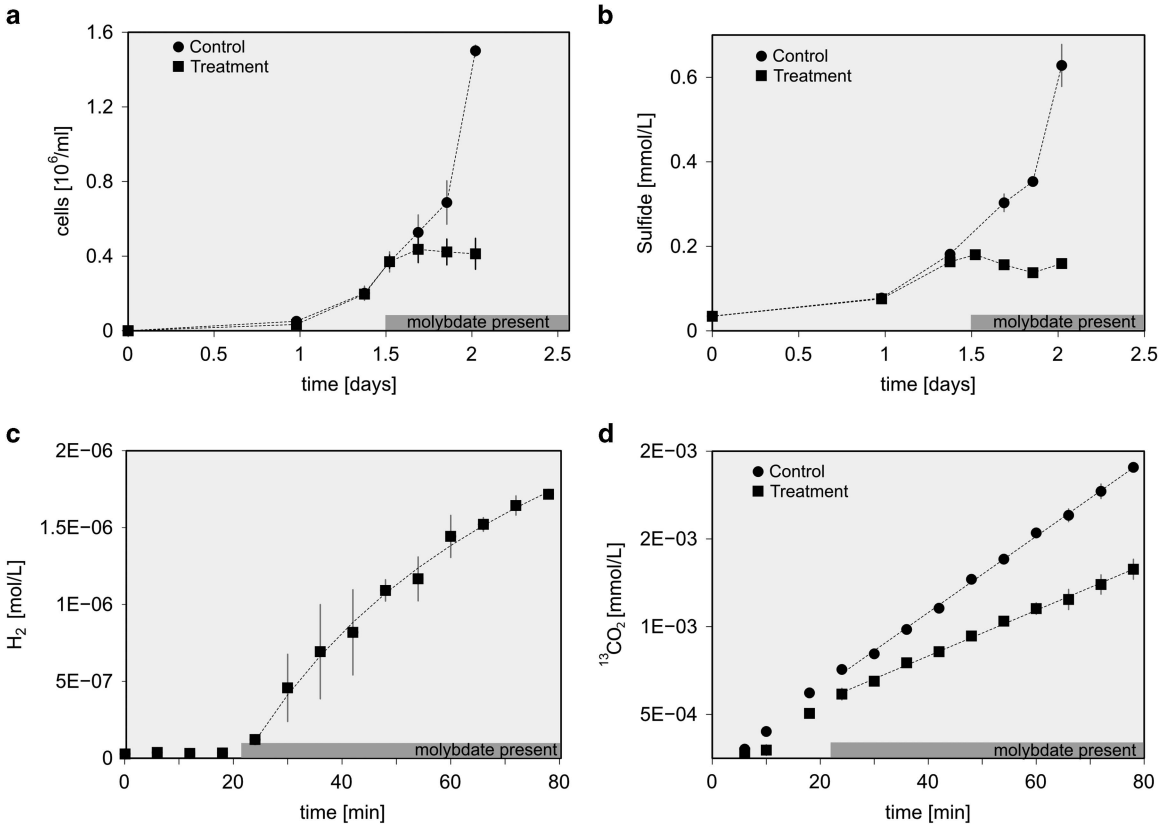

Figure 5 Inhibition of sulfate reduction affects growth of *C. frisia*. (**a** and **b**) Cell numbers and sulfide production in cultures of *C. frisia* in which sulfate reduction was inhibited (squares) compared to controls in which sulfate reduction was active (circles). (**c** and **d**) Hydrogen production and $^{13}CO_2$ production rates before and after inhibition of sulfate reduction. (**d**) Sulfate reduction was inhibited by the addition of molybdate (see gray bar). For each treatment, two parallel cultures were grown. The error bars represent range.

which are growth inhibitors at elevated concentrations (Maiorella *et al.,* 1983). The removal of inhibitory metabolic byproducts by Deltaproteobacteria therefore provides an important fitness benefit to *C. frisia*.

The second major metabolic function performed by the bacteria co-enriched with *C. frisia* appeared to be the degradation of incompletely digested, macromolecular organic material. Microscopic imaging showed that this material originated from fecal pellets excreted by *C. frisia*. As we did not provide any organic carbon other than prey bacteria to our enrichment, this material likely represented a major carbon source for bacterial growth. This also explains the high abundance of bacterial species in our enrichment that are adapted to use this type of material. Bacteroidetes are known as consumers of macromolecules (Fernández-Gómez *et al.*, 2013) and were inferred to use detritus as their substrates. The presence and activity of the two populations of Firmicutes also suggested the availability of smaller organic molecules such as oligopeptides, amino acids and sugars. These might be released either directly by *C. frisia*, or during the hydrolysis of proteins and polysaccharides by Bacteroidetes. Similar niche partitioning between Bacteroidetes and Firmicutes is known for many other organic carbon-rich environments (for example, the digestive tract of animals (Lozupone *et al.*, 2012) or marine oxygen minimum zones (Wright *et al.*, 2012)). The processing of organic waste products by Bacteroidetes and Firmicutes is, therefore, in good agreement with the known physiological capabilities of these species.

A typical characteristic for syntrophic bacterial communities is the formation of multispecies aggregates. Aggregate formation can enhance the exchange of metabolites between different populations, thereby accelerating fermentative reactions and degradation of organic material (Schink and Thauer, 1988). In our enrichment, aggregates most likely arose from bacterial colonization of detritus excreted by *C. frisia*. As *C. frisia* was often directly associated to these aggregates, it could likely benefit from the high turnover of hydrogen and other metabolites within these aggregates. In addition, *C. frisia* may benefit from an increased availability of prey bacteria in aggregates. This way, excretion of detritus by *C. frisia* and the subsequent bacterial colonization of this material, can be interpreted as a primitive form of microbial agriculture.

It will be an interesting research avenue, to address how widespread similar bi-directional

metabolic interactions between predatory flagellates and bacteria are in the environment. To date, there are many reported cases of specific protists-bacterial co-occurrences, which may be a result of metabolic interdependencies. For example, community fingerprinting by 16S rDNA amplicon sequencing showed that a bloom of *Carpediemonas* and related *Diplomonads* was accompanied by a specific enrichment for Bacteroidetes, Firmicutes and known sulfate-reducing Deltaproteobacteria (Holmes *et al.*, 2013). Another study based on single-cell sequencing of flow-sorted planktonic eukaryotes showed that Firmicutes and Deltaproteobacteria are preferentially associated with heterotrophic protists (Martinez-Garcia *et al.*, 2012). So far, a common assumption is that an enrichment of specific prokaryotic phenotypes stimulates the growth of flagellates that are adapted to prey on these species (Pernthaler, 2005; Holmes *et al.*, 2013). The results presented here, however, show that for anoxic environments, the opposite provides an equally compelling explanation—predatory microbial eukaryotes can also stimulate the growth of specific prokaryotic populations, which are adapted to consume their metabolic waste products.

In conclusion, we have shown that *C. frisia* is a newly identified anerobic flagellate, that likely engages in a hydrogen- and organic carbon-based metabolic syntrophy with sulfate-reducing Deltaproteobacteria. This syntrophy appears to benefit *C. frisia* by removing inhibitory metabolites and by creating a biochemical environment that promotes fermentative hydrogen production. In return, *C. frisia* appears to provide its associated microbiota with predigested organic macromolecules, sugars, organic acids and hydrogen. The described metabolic interdependences provide a framework to predict the ecological importance of specific co-occurrences between heterotrophic microbial eukaryotes and prokaryotic populations. In addition, the results show that the concept of metabolic syntrophy, as a form of microbial mutualism, can also apply for inter-kingdom interactions between anaerobic flagellates and free-living prokaryotes.

Genus Carpediemonas Ekebom et al. 1996

Carpediemonas frisia sp. nov. Hamann et al. 2017

Description. *Carpediemonas frisia* is a flagellated marine protist with characteristics of the genus (Simpson and Patterson, 1999). The cells are typically around 5 μm long, pear-shaped, slightly compressed laterally, with two flagella of unequal length. Starving cells can be as small as 3 μm. Flagella emerge from the anterior end of the ventral groove. The anterior flagellum is about 5 μm long. The posterior flagellum is two to three times longer and has a thickened, shuffle-like morphology near its origin. The anterior flagellum performs a sweeping motion, bending its tip backwards. In swimming cells, the longer posterior flagellum beats and provides additional motive force. The cells preferentially swim along surfaces, holding the anterior side in contact with the substrate. Small filamentous pseudopodia emerge from all parts of the cell. No cysts are observed. *C. frisia* is differentiated from *Carpediemonas membranifera* by the presence of mitochondria-related organelles with slight membrane folding.

Habitat. This species was isolated from marine tidal flat sediment collected from a sulfidic sediment layer. The sampling site is commonly known as 'Janssand' and located in the German Wadden Sea south of the island Spiekeroog (53.73585 N, 7.69905 E).

Etymology. The species name frisia is Latin and refers to the coastal region of the southeastern North Sea 'Friesland', which is the historical settlement area of the Friesians.

Gene sequence data. The nearly complete SSU rRNA gene of this isolate (strain S16) is deposited in GenBank under accession no. KY031954.

Conflict of Interest

The authors declare no conflict of interest.

Acknowledgements

We thank Theresa Hargesheimer, Lulu Liu, Gabi Klockgether, Ramona Appel and Ines Kattelmann for technical assistance, Xiaoli Dong for her help with metagenomics and Alastair Simpson, Ger Strous and Sergio for comments on electron micrographs. We thank Kai-Uwe Hinrichs and Nicole Dubilier for discussions and advice. This study was supported by the European Research Council (ERC) starting grant MASEM 242635 (to MS and EH), the Campus Alberta Innovation Chair Program (to MS and EH), the Canadian Foundation for Innovation (to MS), the German Federal State Nordrhein-Westfalen (to MS), the Max Planck Society and NSERC for a Discovery Grant to MS.

References

Bankevich A, Nurk S, Antipov D, Gurevich AA, Dvorkin M, Kulikov AS *et al.* (2012). SPAdes: a new genome assembly algorithm and its applications to single-cell sequencing. *J Comp Biol* **9**: 455–477.

Bauer M, Kube M, Teeling H, Richter M, Lombardot T, Allers E *et al.* (2006). Whole genome analysis of the marine Bacteroidetes 'Gramella forsetii" reveals adaptations to degradation of polymeric organic matter. *Environ Microbiol* **8**: 2201–2213.

Boxma B, de Graaf R, Staay GWM, Alen TA, Ricard G, Gabaldon T *et al.* (2005). An anaerobic mitochondrion that produces hydrogen. *Nature* **434**: 72–74.

van Bruggen JJA, Stumm CK, Zwart KB, Vogels GD. (1985). Endosymbiotic methanogenic bacteria of the sapropelic amoeba Mastigella. *FEMS Microbiol Ecol* **1**: 187–192.

Cantarel BL, Korf I, Robb SMC, Parra G, Ross E, Moore B *et al.* (2008). MAKER: an easy-to-use annotation pipeline designed for emerging model organism genomes. *Genome Res* **18**: 188–196.

Dyksma S, Bischof K, Fuchs BM, Hoffmann K, Meier D, Meyerdierks A *et al.* (2016). Ubiquitous Gammaproteobacteria dominate dark carbon fixation in coastal sediments. *ISME J* **10**: 1939–1953.

Edgcomb VP (2016). Marine protist associations and environmental impacts across trophic levels in the twilight zone and below. *Curr Opin Microbiol* **31**: 169–175.

Edgcomb VP, Kysela DT, Teske A, de Vera Gomez A, Sogin ML. (2002). Benthic eukaryotic diversity in the Guaymas Basin hydrothermal vent environment. *Proc Natl Acad Sci USA* **99**: 7658–7662.

Emanuelsson O, Brunak S, vonHeijne G, Nielsen H. (2007). Locating proteins in the cell using TargetP, SignalP, and related tools. *Nat Protoc* **2**: 953–971.

Fernández-Gómez B, Richter M, Schüler M, Pinhassi J, Acinas SG, González JM *et al.* (2013). Ecology of marine Bacteroidetes: a comparative genomics approach. *ISME J* **7**: 1026–1037.

Fenchel TM, Jørgensen BB. (1977). Detritus food chains of aquatic ecosystems: the role of bacteria. In: Alexander M (ed), *Advances in Microbial Ecology*. Plenum Press: New York, NY, USA, pp 1–58.

Finn RD, Bateman A, Clements J, Coggill P, Eberhardt RY, Eddy SR *et al.* (2014). Pfam: the protein families database. *Nucleic Acids Res* **42**: D222–D230.

Finn RD, Clements J, Arndt W, Miller BL, Wheeler TJ, Schreiber F *et al.* (2015). HMMER web server: 2015 update. *Nucleic Acids Res* **43**: W30–W38.

García-Martínez J, Acinas SG, Massana R, Rodríguez-Valera F. (2002). Prevalence and microdiversity of Alteromonas macleodii-like microorganisms in different oceanic regions. *Environ Microbiol* **4**: 42–50.

Gittel A, Mußmann M, Sass H, Cypionka H, Könneke M. (2008). Identity and abundance of active sulphate-reducing bacteria in deep tidal flat sediments determined by directed cultivation and CARD-FISH analysis. *Environ Microbiol* **10**: 2645–2658.

Glass EM, Wilkening J, Wilke A, Antonopoulos D, Meyer F. (2010). Using the metagenomics RAST server (MG-RAST) for analyzing shotgun metagenomes. *Cold Spring Harb Protoc* **5**: e-pub ahead of print; doi:10.1101/pdb.prot5368.

Glud RN (2008). Oxygen dynamics of marine sediments. *Mar Biol Res* **4**: 243–289.

Hamann E, Gruber-Vodicka H, Kleiner M, Tegetmeyer HE, Riedel D, Littmann S *et al.* (2016). Environmental Breviatea harbour mutualistic Arcobacter epibionts. *Nature* **534**: 254–258.

van Hoek AH, van Alen TA, Sprakel VS, Leunissen JA, Brigge T, Vogels GD *et al.* (2000). Multiple acquisition of methanogenic archaeal symbionts by anaerobic ciliates. *Mol Biol Evol* **17**: 251–258.

Holmes DE, Giloteaux L, Williams KH, Wrighton KC, Wilkins MJ, Thompson CA *et al.* (2013). Enrichment of specific protozoan populations during *in situ* bioremediation of uranium-contaminated groundwater. *ISME J* **7**: 1286–1298.

Katoh K, Standley DM. (2013). MAFFT multiple sequence alignment software version 7: improvements in performance and usability. *Mol Biol Evol* **30**: 772–780.

Korf I (2004). Gene finding in novel genomes. *BMC Bioinformatics* **5**: 59.

Leggett RM, Clavijo BJ, Clissold L, Clark MD, Caccamo M. (2014). Next clip: an analysis and read preparation tool for nextera long mate pair libraries. *Bioinformatics* **30**: 566–568.

Letunic I, Doerks T, Bork P (2015). SMART: Recent updates, new developments and status in 2015. *Nucleic Acids Res* **43**: D257–D260.

Lozupone CA, Stombaugh JI, Gordon JI, Jansson JK, Knight R. (2012). Diversity, stability and resilience of the human gut microbiota. *Nature* **489**: 220–230.

Maiorella B, Blanch HW, Wilke CR. (1983). By-product inhibition effects on ethanolic fermentation by Saccharomyces cerevisiae. *Biotechnol Bioeng* **25**: 103–121.

Martinez-Garcia M, Brazel D, Poulton NJ, Swan BK, Gomez ML, Masland D *et al.* (2012). Unveiling *in situ* interactions between marine protists and bacteria through single cell sequencing. *ISME J* **6**: 703.

McInerney MJ, Rohlin L, Mouttaki H, Kim U, Krupp RS, Rios-Hernandez L *et al.* (2007). The genome of Syntrophus aciditrophicus: life at the thermodynamic limit of microbial growth. *Proc Natl Acad Sci USA* **104**: 7600–7605.

Müller M, Mentel M, van Hellemond JJ, Henze K, Woehle C, Gould SB *et al.* (2012). Biochemistry and evolution of anaerobic energy metabolism in eukaryotes. *Microbiol Mol Biol Rev* **76**: 444–495.

Ohkuma M, Noda S, Hattori S, Iida T, Yuki M, Starns D *et al.* (2015). Acetogenesis from H2 plus CO2 and nitrogen fixation by an endosymbiotic spirochete of a termite-gut cellulolytic protist. *Proc Natl Acad Sci USA* **698**: 201423979.

Oremland RS, Capone DG. (1988). Use of specific inhibitors in biogeochemistry and microbial ecology. *Adv Microb Ecol* **10**: 285–383.

Parks DH, Imelfort M, Skennerton CT, Hugenholtz P, Tyson GW. (2015). CheckM: assessing the quality of microbial genomes recovered from isolates, single cells, and metagenomes. *Genome Res* **25**: 1043–1055.

Pernthaler J. (2005). Predation on prokaryotes in the water column and its ecological implications. *Nat Rev Microbiol* **3**: 537–546.

Schink B, Thauer RK. (1988). Energetics of syntrophic methane formation and the influence of aggregation. In: Lettinga G, Zehnder AJB, Grotenhuis JTC, Hulshoff LW (eds), Granular anaerobic sludge: microbiology and technology. Pudoc: Wageningen, The Netherlands, pp 5–17.

Schut GJ, Adams MWW. (2009). The iron-hydrogenase of Thermotoga maritima utilizes ferredoxin and NADH synergistically: a new perspective on anaerobic hydrogen production. *J Bacteriol* **191**: 4451–4457.

Sherr EB, Sherr BF. (2002). Significance of predation by protists in aquatic microbial food webs. *Antonie Van Leeuwenhoek* **81**: 293–308.

Sieber JR, McInerney MJ, Gunsalus RP. (2012). Genomic insights into syntrophy: the paradigm for anaerobic metabolic cooperation. *Annu Rev Microbiol* **66**: 429–452.

Simpson AGB, Patterson DJ. (1999). The ultrastructure of Carpediemonas membranifera (Eukaryota) with reference to the 'excavate hypothesis'. *Eur J Protistol* **35**: 353–370.

Smit A, Hubley R, Green P. (2013), RepeatMasker Open-4.0. 2013–2015. Available at http://www.repeatmasker.org.

Smith CJ, Nedwell DB, Dong LF, Osborn AM. (2007). Diversity and abundance of nitrate reductase genes (narG and napA), nitrite reductase genes (nirS and nrfA),

and their transcripts in estuarine sediments. *Appl Environ Microbiol* **73**: 3612–3622.

Stairs CW, Leger MM, Roger AJ. (2015). Diversity and origins of anaerobic metabolism in mitochondria and related organelles. *Philos Trans R Soc B Lond B Biol Sci* **370**: 20140326.

Stamatakis A. (2014). RAxML version 8: a tool for phylogenetic analysis and post-analysis of large phylogenies. *Bioinformatics* **30**: 1312–1313.

Stams AJM, Plugge CM. (2009). Electron transfer in syntrophic communities of anaerobic bacteria and archaea. *Nat Rev Microbiol* **7**: 568–577.

Strous M, Kraft B, Bisdorf R, Tegetmeyer HE. (2012). The binning of metagenomic contigs for microbial physiology of mixed cultures. *Front Microbiol* **3**: 410.

Takishita K, Kolisko M, Komatsuzaki H, Yabuki A, Inagaki Y, Cepicka I *et al.* (2012). Multigene phylogenies of diverse carpediemonas-like organisms identify the closest relatives of 'Amitochondriate" Diplomonads and Retortamonads. *Protist* **163**: 344–355.

Ter-Hovhannisyan V, Lomsadze A, Chernoff YO, Borodovsky M. (2008). Gene prediction in novel fungal genomes using an *ab initio* algorithm with unsupervised training. *Genome Res* **18**: 1979–1990.

Waters E, Hohn MJ, Ahel I, Graham DE, Adams MD, Barnstead M *et al.* (2003). The genome of Nanoarchaeum equitans: insights into early archaeal evolution and derived parasitism. *Proc Natl Acad Sci USA* **100**: 12984–12988.

Wright JJ, Konwar KM, Hallam SJ. (2012). Microbial ecology of expanding oxygen minimum zones. *Nat Rev Microbiol* **10**: 381–394.

Wylezich C, Jürgens K. (2011). Protist diversity in suboxic and sulfidic waters of the Black Sea. *Environ Microbiol* **13**: 2939–2956.

Supplementary Information accompanies this paper on The ISME Journal website (http://www.nature.com/ismej)